

# Shear viscosity and out of equilibrium dynamics

Andrej El<sup>1,\*</sup>, Azwinndini Muronga<sup>2,†</sup>, Zhe Xu<sup>1,‡</sup>, Carsten Greiner<sup>1,§</sup>

<sup>1</sup> *Institut für Theoretische Physik, Goethe-Universität Frankfurt,  
Max-von-Laue Strasse 1, D-60438, Frankfurt am Main, Germany and*

<sup>2</sup> *Institute for Theoretical Physics and Astrophysics,  
Department of Physics, University of Cape Town, Rondebosch 7701,  
South Africa; UCT-CERN Research Centre, Department of Physics,  
University of Cape Town, Rondebosch 7701, South Africa*

## Abstract

Using Grad's method, we calculate the entropy production and derive a formula for the second-order shear viscosity coefficient in a one-dimensionally expanding particle system, which can also be considered out of chemical equilibrium. For a one-dimensional expansion of gluon matter with Bjorken boost invariance, the shear tensor and the shear viscosity to entropy density ratio  $\eta/s$  are numerically calculated by an iterative and self-consistent prescription within the second-order Israel-Stewart hydrodynamics and by a microscopic parton cascade transport theory. Compared with  $\eta/s$  obtained using the Navier-Stokes approximation, the present result is about 20% larger at a QCD coupling  $\alpha_s \sim 0.3$  (with  $\eta/s \approx 0.18$ ) and is a factor of 2 – 3 larger at a small coupling  $\alpha_s \sim 0.01$ . We demonstrate an agreement between the viscous hydrodynamic calculations and the microscopic transport results on  $\eta/s$ , except when employing a small  $\alpha_s$ . On the other hand, we demonstrate that for such small  $\alpha_s$ , the gluon system is far from kinetic and chemical equilibrium, which indicates the break down of second-order hydrodynamics because of the strong nonequilibrium evolution. In addition, for large  $\alpha_s$  (0.3 – 0.6), the Israel-Stewart hydrodynamics formally breaks down at large momentum  $p_T \gtrsim 3$  GeV but is still a reasonably good approximation.

PACS numbers: 24.10.Lx, 24.10.Nz, 12.38.Mh, 25.75.-q, 05.60.-k

---

\* el@th.physik.uni-frankfurt.de

† Azwinndini.Muronga@uct.ac.za

‡ xu@th.physik.uni-frankfurt.de

§ Carsten.Greiner@th.physik.uni-frankfurt.de

## I. INTRODUCTION

Recent experimental measurements on the elliptic flow parameter  $v_2$  at the BNL Relativistic Heavy Ion Collider (RHIC) [1, 2, 3] show a strong collectivity of the deconfined quark-gluon matter. The matter produced was thus specified as a strongly coupled quark-gluon plasma (sQGP) [4, 5, 6] or as a perfect fluid [7]. Further attempts to determine how imperfect the sQGP really is have drawn attention to transport coefficients like viscosity [8, 9, 10, 11, 12, 13, 14, 15, 16] and to the derivation and solution of viscous hydrodynamics [17, 18, 19, 20, 21, 22, 23, 24], which is still a mathematical challenge.

Most current viscous hydrodynamic equations are based on second-order Israel-Stewart kinetic theory [25]. They are solved numerically using the given viscosity coefficients and initial conditions as well as parton and hadron equation of state. In particular, the shear viscosity to entropy density ratio  $\eta/s$  is determined by comparing the elliptic flow from the viscous hydrodynamical calculations with the data at RHIC, as has been done recently in Refs. [26, 27], where the value  $\eta/s \approx 0.1$  was obtained. On the other hand, even though the early partonic phase may be well described by ideal hydrodynamics ( $\eta = 0$ ), the hadronic afterburning [28] has a larger dissipative effect, which may be enough to slow down the generation of the elliptic flow and bring its final value into agreement with the data.

Dissipative phenomena can be alternatively described in transport calculations solving Boltzmann equations of matter constituents [29, 30, 31, 32, 33, 34, 35, 36]. This approach is applicable for investigations of such phenomena as thermalization, kinetic decoupling, and dynamics of high-energy particles in systems far from equilibrium, i.e., in a regime where the second-order viscous hydrodynamics breaks down [37].

Recently, an on-shell parton cascade Boltzmann Approach of MultiParton Scatterings (BAMPS) has been developed to study thermalization [34, 38, 39], elliptic flow  $v_2$  [40, 41, 42], and the energy loss [43] of gluons produced in Au+Au collisions at RHIC energy. Also the generation and evolution of viscous shock waves are surprisingly well realized in BAMPS calculations [44]. The shear viscosity of the gluon matter at RHIC has been estimated from BAMPS calculations [41, 42] within the Navier-Stokes approximation [12]. The authors found that to produce large  $v_2$  comparable with the experimental data, the gluon matter should have an  $\eta/s$  between 0.08 and 0.2 constrained by details of the hadronization and the kinetic freeze out. This is in line with the dissipative hydrodynamic approach [26].

Perturbative QCD (pQCD) gluon bremsstrahlung  $gg \leftrightarrow ggg$  is responsible for the low  $\eta/s$  ratio and for the generation of large elliptic flow.

Beyond the Navier-Stokes approximation, which has been used in Refs.[11, 12], we derive a new microscopic formula for the shear viscosity coefficient from the kinetic theory using the second-order Grad's method. This is one of the goals in the present article. The derivation follows Ref. [45] and is generalized for a particle system out of chemical equilibrium.

Another goal is to elaborate on the breakdown region of the second-order viscous hydrodynamics. To do this we investigate the time evolution of a gluon matter in a one-dimensional expansion with Bjorken boost invariance [46] by solving the Israel-Stewart hydrodynamic equations [37] as well as by performing similar BAMPS transport calculations for comparison. We quantify the deviation of the gluon distribution function from kinetic equilibrium and show the region with large deviation, where the applicability of the Israel-Stewart hydrodynamics is questionable.

The article is organized as follows. In Sec. II we introduce theoretical framework for deriving viscosity from the kinetic theory using second-order Grad's method. We consider a massless particle system, which undergoes a one-dimensional expansion with Bjorken boost invariance. A comparison with the results obtained by the Navier-Stokes approximation [12] is given in Sec. III. Using the formula derived in Sec. II we calculate the shear viscosity to entropy density ratio  $\eta/s$  of gluon matter: in Sec. IV an iterative and self-consistent approach is introduced to calculate  $\eta/s$  from the Israel-Stewart hydrodynamics, whereas the results from BAMPS calculations are presented in Sec. V. For both hydrodynamic and transport calculations, deviations from kinetic as well as chemical equilibrium are shown and analyzed. Conclusions are given in Sec. VI.

## II. SHEAR VISCOSITY COEFFICIENT FROM SECOND-ORDER KINETIC THEORY

Relativistic causal dissipative hydrodynamic equations can be derived from the kinetic theory by applying Grad's method of moments [47]. A detailed derivation is reported in Refs. [45, 48] and a prescription for calculating transport coefficients is also given there. In this section we will follow Ref. [45] to derive an expression for the shear viscosity coefficient  $\eta$  when the considered system is out of chemical equilibrium.

The basic equation of relativistic kinetic theory is the Boltzmann equation

$$p^\mu \partial_\mu f(x, p) = C[f(x, p)] \quad (1)$$

for a one-particle phase-space distribution function  $f(x, p) = \frac{dN}{\frac{1}{(2\pi)^3} d^3p d^3x}$ .  $C[f(x, p)]$  denotes the collision term, which accounts for all microscopic interaction processes among particles. The entropy four-current is defined by [45, 49]

$$s^\mu = - \int \frac{d^3p}{(2\pi)^3 p^0} p^\mu f(x, p) [\ln(f(x, p)) - 1]. \quad (2)$$

The entropy production is then given by

$$\partial_\mu s^\mu = - \int dw p^\mu \partial_\mu f(x, p) \ln f(x, p) = - \int dw C[f(x, p)] \ln f(x, p) \quad (3)$$

with the short notation  $dw = \frac{d^3p}{(2\pi)^3 p^0}$ .

We now assume that the deviation of  $f(x, p)$  from the equilibrium distribution  $f_{eq}(x, p)$  is small:

$$f(x, p) = f_{eq}(x, p) (1 + \phi(x, p)) \quad (4)$$

where  $\phi(x, p) \ll 1$  and

$$f_{eq}(x, p) = \lambda e^{-\frac{u_\mu p^\mu}{T}}. \quad (5)$$

$\lambda(x)$  and  $T(x)$  denote the local fugacity and temperature, respectively.  $u^\mu(x)$  is the hydrodynamic four-velocity of the medium. Equation (5) is the standard form for Boltzmann particles. The derivation below can be easily extended for Bose and Fermi particles. In addition, we will restrict the following discussions to the case of massless particles (e.g., gluons).

We expand  $\phi(x, p)$  up to second order in momentum, that is,

$$\phi(x, p) = \epsilon(x) - \epsilon_\mu(x) p^\mu + \epsilon_{\mu\nu}(x) p^\mu p^\nu, \quad (6)$$

where the momentum-independent coefficients can be expressed in terms of the dissipative currents  $\Pi$ ,  $q^\mu$  and  $\pi^{\mu\nu}$  denoting bulk pressure, heat flux and shear tensor [45, 48]:

$$\epsilon_{\mu\nu} = A_2(3u_\mu u_\nu - \Delta_{\mu\nu})\Pi - B_1 u_{(\mu} q_{\nu)} + C_0 \pi_{\mu\nu} \quad (7)$$

$$\epsilon_\mu = A_1 u_\mu \Pi - B_0 q_\mu \quad (8)$$

$$\epsilon = A_0 \Pi \quad (9)$$

with the projector  $\Delta^{\mu\nu} = g^{\mu\nu} - u^\mu u^\nu$  and symmetrization operation  $u_{(\mu} q_{\nu)} = \frac{1}{2}(u_\mu q_\nu + u_\nu q_\mu)$ . The metric used in this work is  $g^{\mu\nu} = \text{diag}(1, -1, -1, -1)$ . In general, the dissipative fluxes are defined as projections of deviations of the energy-momentum tensor  $T^{\mu\nu}$  and particle four-current  $N^\mu$  from their equilibrium form [45, 48]:

$$\Pi = -\frac{1}{3}\Delta_{\mu\nu}\delta T^{\mu\nu} \quad (10)$$

$$q^\mu = \Delta_\nu^\mu u_\rho \delta T^{\rho\nu} - \frac{4}{3}\Delta_\nu^\mu \delta N^\nu \quad (11)$$

$$\pi^{\mu\nu} = \delta T^{<\mu\nu>} = \left( \frac{1}{2}\Delta_\alpha^\mu \Delta_\beta^\nu + \frac{1}{2}\Delta_\alpha^\nu \Delta_\beta^\mu - \frac{1}{3}\Delta_{\alpha\beta}\Delta^{\mu\nu} \right) \delta T^{\alpha\beta} \quad (12)$$

with the definitions  $N^\mu = \int dp p^\mu f$ ,  $T^{\mu\nu} = \int dp p^\mu p^\nu f$  and  $\delta T^{\mu\nu} = T^{\mu\nu} - T_{eq}^{\mu\nu}$ ,  $\delta N^\mu = N^\mu - N_{eq}^\mu$ .

We use the following local matching conditions on the energy and particle densities:

$$e = e_{eq} = \frac{3\lambda T^4}{\pi^2} \quad (13)$$

$$n = n_{eq} = \frac{\lambda T^3}{\pi^2} \quad (14)$$

with the definitions for the densities  $e = u_\mu T^{\mu\nu} u_\nu$  and  $n = u_\mu N^\mu$ . The local temperature simply follows as  $T = e/3n$ . The fugacity is then calculated via  $\lambda = n/(\frac{1}{\pi^2}T^3)$ . One obtains immediately  $u_\mu \delta T^{\mu\nu} u_\nu = 0$  and  $u_\mu \delta N^\mu = 0$ . The bulk pressure  $\Pi$  from Eq. (10) then becomes

$$\Pi \sim (g_{\mu\nu} - u_\mu u_\nu) \delta T^{\mu\nu} = \delta T^\nu_\nu = 0 \quad (15)$$

for massless particles, since the energy momentum tensor is traceless in this case. Thus,  $\epsilon = 0$  according to Eq. (9).

In the following, we will consider a one-dimensional Bjorken expansion [46]. This implies that in the local rest frame, the distribution function  $f(x, p)$  is symmetric when transforming  $\vec{p}$  to  $-\vec{p}$ . Thus in the local rest frame,  $T^{0i} = 0$  and  $N^i = 0$ , where  $i = 1, 2, 3$ . The heat flux  $q^\mu$  (11) vanishes in the local rest frame because

$$q^\mu = g_\nu^\mu u_\rho \delta T^{\rho\nu} - u^\mu u_\nu \delta T^{\rho\nu} - \frac{4}{3}g_\nu^\mu \delta N^\nu + \frac{4}{3}u^\mu u_\nu \delta N^\nu = u_\rho \delta T^{\rho\mu} - \frac{4}{3}\delta N^\mu = 0. \quad (16)$$

We obtain then  $\epsilon_\mu p^\mu \sim q_\mu p^\mu = 0$  [see Eq. (9)].

For a one-dimensionally expanding system, Eq. (6) thus reduces to

$$\phi(x, p) = \epsilon_{\mu\nu}(x) p^\mu p^\nu. \quad (17)$$

Putting  $f = f_{eq}(1 + \phi)$  into Eq. (3) and using the linearization

$$\ln(1 + \phi) \approx \phi = \epsilon_{\mu\nu}(x)p^\mu p^\nu \quad (18)$$

we rewrite Eq.(3) as

$$\partial_\mu s^\mu = - \int dw C[f(x, p)] \ln f_{eq}(x, p) - \int dw C[f(x, p)] \epsilon_{\mu\nu} p^\mu p^\nu \quad (19)$$

Using the formula (5) for  $f_{eq}$  in the first term of Eq. (19) one has

$$\begin{aligned} & - \int dw C[f(x, p)] \ln f_{eq}(x, p) = - \int dw C[f(x, p)] (\ln \lambda - u_\mu p^\mu / T) \\ & = - \ln \lambda \int dw C[f(x, p)] + u_\mu \int dw p^\mu C[f(x, p)] / T \\ & = - \ln \lambda \int dw C[f(x, p)] = - \ln \lambda \partial_\mu N^\mu . \end{aligned} \quad (20)$$

For the second-last identity in Eq. (20), we used the energy-momentum conservation:  $\int dw p^\nu C[f(x, p)] = \partial_\mu \int dw p^\nu p^\mu f = \partial_\mu T^{\nu\mu} = 0$ . Equation (20) describes entropy production due to particle production ( $\partial_\mu N^\mu > 0$  for  $\lambda < 1$ ) and absorption ( $\partial_\mu N^\mu < 0$  for  $\lambda > 1$ ).

With the definitions

$$P^{\mu\nu} = \int dw p^\mu p^\nu C[f(x, p)] \quad (21)$$

$$\bar{C} = \int dw C[f(x, p)] = \partial_\mu N^\mu , \quad (22)$$

which are the 2nd and the 0th moment of the collision term the entropy production in Eq.(19) can be now written in a more compact form

$$\partial_\mu s^\mu = -\bar{C} \ln \lambda - \epsilon_{\mu\nu} P^{\mu\nu} . \quad (23)$$

In general, the entropy production in an imperfect fluid can be expressed by the positive definite form [25, 50, 51]

$$\partial_\mu s^\mu = -J \ln \lambda + (\zeta T)^{-1} \Pi^2 - (\kappa T)^{-1} q_\alpha q^\alpha + (2\eta T)^{-1} \pi_{\alpha\beta} \pi^{\alpha\beta} , \quad (24)$$

where  $\zeta$ ,  $\kappa$ , and  $\eta$  are non-negative coefficients denoting the bulk viscosity, heat conductivity and shear viscosity, respectively.  $J = \partial_\mu N^\mu$  is the source of particle production [50, 51] and is identical with  $\bar{C}$  (22). For a chemically equilibrated system  $J$  vanishes. Comparing Eq. (23) to (24) we find

$$- \epsilon_{\mu\nu} P^{\mu\nu} = (2\eta T)^{-1} \pi_{\alpha\beta} \pi^{\alpha\beta} , \quad (25)$$

because in our case  $\Pi = 0$  and  $q_\alpha q^\alpha = 0$  as discussed above. The expression (25) is exactly the same as obtained in [45] and describes entropy production due to shear viscous effects.

We then obtain the final expression for the shear viscosity coefficient

$$\eta = -\frac{\pi_{\alpha\beta}\bar{\pi}^{\alpha\beta}}{2T\epsilon_{\mu\nu}P^{\mu\nu}} = -\frac{\pi_{\alpha\beta}\bar{\pi}^{\alpha\beta}}{2TC_0\pi_{\mu\nu}P^{\mu\nu}}. \quad (26)$$

The last identity is due to the fact that  $q^\mu$  vanishes in the local rest frame and thus  $u_{(\mu}q_{\nu)}P^{\mu\nu} = 0$ . We note that the derived formula (26) is an approximate expression of the true shear viscosity. We call the ‘‘second-order’’ shear viscosity, because we have used terms up to second order in momentum for  $\phi(x, p)$  [see Eq. (6)].

To calculate  $C_0$  we go to the local rest frame, i.e.,  $u^\mu = (1, 0, 0, 0)$ , where

$$\pi^{\mu\nu} = \delta T^{\mu\nu} = T^{\mu\nu} - T_{eq}^{\mu\nu} = \epsilon_{\alpha\beta} \int dw p^\mu p^\nu p^\alpha p^\beta f_{eq}(x, p) \quad (27)$$

is valid according to Eqs. (12) and (17) for a (0+1) dimensional expansion. In this frame  $\epsilon_{\alpha\beta}$  [see Eq. (7)] reduces to

$$\epsilon_{\alpha\beta} = C_0 \pi_{\alpha\beta}. \quad (28)$$

Calculating the integrals in Eq. (27) with  $f_{eq} = \lambda e^{-E/T}$  gives

$$(1 - C_0 40\lambda T^6 / \pi^2) \pi^{0j} = 0, \quad j = 1, 2, 3 \quad (29)$$

$$(1 - C_0 8\lambda T^6 / \pi^2) \pi^{ij} = 0, \quad i, j = 1, 2, 3. \quad (30)$$

We have used the fact that  $\pi^{\mu\nu}$  is traceless and  $\pi^{00} = 0$  due to the matching condition (13) and  $T^{00} = e$  in the local rest frame. For a system undergoing a one-dimensional Bjorken expansion, i.e., in a (0+1) dimensional case, all off-diagonal elements of  $T^{\mu\nu}$  - and thus  $\pi^{\mu\nu}$  as well - vanish in the local rest frame, particularly  $T^{0j} = \pi^{0j} = 0, j = 1, 2, 3$ . Thus we obtain

$$C_0 = \frac{\pi^2}{8\lambda T^6}. \quad (31)$$

If the third spatial coordinate is chosen as the expansion axis, we have  $T^{11} = T^{22}$ , and in the local rest frame the shear tensor takes the form

$$\pi^{\mu\nu} = \begin{pmatrix} 0 & 0 & 0 & 0 \\ 0 & -\frac{\bar{\pi}}{2} & 0 & 0 \\ 0 & 0 & -\frac{\bar{\pi}}{2} & 0 \\ 0 & 0 & 0 & \bar{\pi} \end{pmatrix} \quad (32)$$

which is also given in [51]. We thus obtain

$$\pi_{\mu\nu}\pi^{\mu\nu} = \frac{3}{2}\bar{\pi}^2 \quad (33)$$

$$\epsilon_{\mu\nu}P^{\mu\nu} = C_0\pi_{\mu\nu}P^{\mu\nu} = \frac{C_0\bar{\pi}}{2}(3P^{33} - P^{00}), \quad (34)$$

where we have used  $P^{11} + P^{22} = P^{00} - P^{33}$ , because  $P^{\mu\nu}$  is traceless following from the definition (21). Putting Eqs. (27) and (34) into (26) gives the shear viscosity coefficient for a (0+1) dimensionally expanding system of massless particles:

$$\eta = -\frac{3\bar{\pi}}{2TC_0(3P^{33} - P^{00})} = 4n\frac{-T^2\bar{\pi}}{P^{33} - \frac{1}{3}P^{00}}. \quad (35)$$

For the last identity, we have used the matching conditions (14) and Eq. (31).

The energy density  $e$ , the temperature  $T$  and the shear component  $\bar{\pi}$  in a (0+1) dimensional expansion can be calculated by solving viscous hydrodynamic equations with a given value of shear viscosity  $\eta$ . If  $\bar{\pi}$  is known, the distribution function  $f$  is known too [see Eqs. (4), (17) and (28)]. One can thus evaluate  $P^{00}$  and  $P^{33}$  according to their definitions (21). Then  $\eta$  can be calculated employing Eq. (35). In sSec. IV we will introduce an iterative and self-consistent prescription to calculate the second-order shear viscosity.

On the other hand,  $f$  can be obtained by solving the Boltzmann equation (1) directly employing transport simulations. Then  $\eta$  can be easily extracted using Eq. (35). Such calculations will be presented in section V. The results will be compared with those obtained in Sec. IV. As it turns out, a ratio of mean transport free path to expansion time being larger than unity and the variance of  $\phi(x, p)$  being larger than unity will possibly indicate the breakdown of the second-order viscous hydrodynamics. In this regime the validity of (35) is also questionable.

### III. COMPARISON TO SHEAR VISCOSITY FROM NAVIER-STOKES APPROXIMATION

In Ref. [12], the shear viscosity coefficient was derived assuming the Navier-Stokes approximation

$$\pi^{\mu\nu} = 2\eta\nabla^{\langle\mu}u^{\nu\rangle}. \quad (36)$$

It reads

$$\eta_{NS} \cong \frac{1}{5}n\frac{\langle E/3 - p_z^2/E \rangle}{\frac{1}{3} - \langle p_z^2/E^2 \rangle} \frac{1}{\sum R^{\text{tr}} + \frac{3}{4}\partial_t(\ln \lambda)} \quad (37)$$



where

$$\sum R^{\text{tr}} = \frac{\int dw \frac{p_z^2}{E^2} C[f] - \langle p_z^2/E^2 \rangle \int dw C[f]}{n(\frac{1}{3} - \langle p_z^2/E^2 \rangle)} \quad (38)$$

is the total transport collision rate, which was introduced in [38]. All integrals are expressed in the local rest frame.  $\langle \rangle$  denotes the average over particle momentum.

Equation (26) can be used to calculate the shear viscosity if the shear tensor  $\pi_{\mu\nu}$  obeys the Israel-Stewart equation [51]

$$\tau_\pi \Delta_\mu^\alpha \Delta_\nu^\beta \dot{\pi}_{\alpha\beta} + \pi_{\mu\nu} = 2\eta\sigma_{\mu\nu} - \left[ \eta T \partial_\lambda \left( \frac{\tau_\pi}{2\eta T} u^\lambda \right) \pi_{\mu\nu} \right], \quad (39)$$

where  $\sigma_{\mu\nu} = \nabla^{\langle\mu} u^{\nu\rangle}$  and  $\tau_\pi$  denotes the relaxation time [see also Eq. (47) below]. Equation (39) is more general than (36) in the first-order (Navier-Stokes) theory.

If we define

$$\sum R_{\text{Grad}}^{\text{tr}} = \frac{P^{33} - \frac{1}{3}P^{00}}{n(\frac{1}{3}\langle E^2 \rangle - \langle p_z^2 \rangle)}, \quad (40)$$

then the shear viscosity from the Grad's method (35) can be rewritten to

$$\eta_{\text{Grad}} = 4n \frac{T^2 \langle E/3 - p_z^2/E \rangle}{\frac{1}{3}\langle E^2 \rangle - \langle p_z^2 \rangle} \frac{1}{\sum R_{\text{Grad}}^{\text{tr}}}, \quad (41)$$

where we have used  $\bar{\pi} = T^{33} - T_{eq}^{33} = T^{33} - \frac{1}{3}T^{00} = n\langle p_z^2/E - E/3 \rangle$ . Remember that  $P^{\mu\nu}$  is the second moment of the collision term [see Eq. (21)]. The expression (41) is similar to Eq. (37) except for the term  $\frac{3}{4}\partial_t(\ln \lambda)$ , which indicates that chemical equilibration contributes explicitly to the shear viscosity in the Navier-Stokes approximation rather than in the Israel-Stewart approach.

In the next section, we calculate the shear viscosity in a gluon system within the Israel-Stewart approach and compare the result with that obtained using the Navier-Stokes approximation [12].

#### IV. CALCULATION OF SHEAR VISCOSITY IN A GLUON SYSTEM: AN ITERATIVE AND SELF-CONSISTENT PRESCRIPTION

In this section we want to calculate the shear viscosity to the entropy density ratio  $\eta/s$  for a gluonic system, which undergoes a one-dimensional expansion with Bjorken boost invariance, i.e., a (0+1) dimensional expansion.

## A. Prescription

For a (0+1) dimensional case the shear tensor  $\pi_{\mu\nu}$  in the local rest frame is given by Eq. (32). Then the gluon distribution function in the local rest frame reads

$$f(x, p) = \lambda e^{-\frac{E}{T}} [1 - C_0 \bar{\pi} (p_z^2 - p_t^2/2)] \quad (42)$$

according to Eqs. (4), (17), (28) and (32). If  $\bar{\pi}$ ,  $T$  and  $\lambda$  are known, the shear viscosity  $\eta$  can be calculated according to Eq. (35), where  $P^{\mu\nu}$  are evaluated by Eq. (21) via Eq. (42). Note that for the case of a gluonic system the value of  $\eta$  has to be amplified by the degeneracy factor of gluons  $d_G = 16$ . We thus define  $\eta_g = d_G \eta$ . In addition, the gluon entropy density is given by

$$s_g = u_\mu s^\mu = -d_G \int dw p_0 f(x, p) (\ln f(x, p) - 1) \approx (4 - \ln \lambda) n_g - \frac{9\bar{\pi}_g^2}{8n_g T^2}, \quad (43)$$

where  $n_g = d_G \lambda T^3 / \pi^2$  and  $\bar{\pi}_g = d_G \bar{\pi}$  are the gluon number density and the gluon shear component, and we have used the approximation  $\ln(1+\phi) \approx \phi$  for small  $\phi = -C_0 \bar{\pi} (p_z^2 - p_t^2/2)$ . We note that  $\phi$  can be larger than unity for large momenta. In these cases, the expansion [also for Eq. (19)] fails. On the other hand, the distribution function  $f(x, p)$  becomes very small at large momenta. The effect of the invalid expansion on the integrated quantity  $s_g$  is thus negligible at this point.

In principle,  $\phi = (f - f_{eq})/f_{eq}$  gives the relative deviation from kinetic equilibrium. However,  $\phi$  is also a function of momentum. The average  $\langle \phi(x, p) \rangle_{eq}$  over momentum distributed in equilibrium, i.e, using  $f(x, p)$  in zeroth order of  $\bar{\pi}$ , is obviously zero. We introduce the variance  $\sigma_\phi = \sqrt{\langle \phi^2 \rangle_{eq}}$  as the quantity determining the deviation from kinetic equilibrium and we find

$$\sigma_\phi = \frac{9\sqrt{2}}{4} \frac{|\bar{\pi}_g|}{e_g}, \quad (44)$$

where  $e_g = 3n_g T$  is the gluon energy density.

If the deviation from the local kinetic equilibrium is sufficiently small, then the dynamical expansion in a (0+1) dimensional case can be well described by the Israel-Stewart (IS)

viscous hydrodynamic equations [25, 37, 45, 48, 51, 52]:

$$\frac{dn_g}{d\tau} = -\frac{n_g}{\tau}, \quad (45)$$

$$\frac{de_g}{d\tau} = -\frac{4}{3}\frac{e_g}{\tau} + \frac{\bar{\pi}_g}{\tau}, \quad (46)$$

$$\frac{d\bar{\pi}_g}{d\tau} = -\frac{\bar{\pi}_g}{\tau_\pi} - \frac{1}{2}\bar{\pi}_g \left( \frac{1}{\tau} + \frac{1}{\beta_2} T \frac{\partial}{\partial \tau} \left( \frac{\beta_2}{T} \right) \right) + \frac{2}{3} \frac{1}{\beta_2 \tau}, \quad (47)$$

where  $\beta_2 = 9/(4e_g)$  and  $\tau_\pi = 2\beta_2\eta_g$  denotes the relaxation time. Equation (47) is just Eq. (39) expressed in the local rest frame using the hydrodynamic velocity  $u^\mu = \frac{1}{\tau}(t, 0, 0, z)$ , where  $\tau = \sqrt{t^2 - z^2}$ . In derivation of Eq. (39), which is discussed in Ref. [51], only terms of second order in gradients and dissipative flux  $\pi_{\mu\nu}$  have been included. If  $\sigma_\phi$  in Eq. (44) is larger than unity, further terms containing  $\sigma_\phi^2 \sim (\bar{\pi}/e)^2 \sim (\beta_2\bar{\pi})^2$  are no longer small enough anymore to be omitted in derivation of Eq. (39) and thus in Eq. (47) as well, i.e., a higher order hydrodynamic equation is needed. Thus the value of  $\sigma_\phi$  is an indicator for a breakdown of second-order hydrodynamic theory.

Equation (45) for the gluon density can be easily solved:

$$n_g(\tau) = n_g(\tau_0) \frac{\tau_0}{\tau}, \quad (48)$$

which is identical with the result from ideal hydrodynamics. On the other hand, the energy density decreases slower than in ideal hydrodynamics due to the viscous effects:

$$e_g(\tau) = e_g(\tau_0) \left( \frac{\tau_0}{\tau} \right)^\xi, \quad \xi \leq \frac{4}{3}. \quad (49)$$

Thus we obtain the gluon fugacity

$$\lambda(\tau) = \frac{n_g(\tau)}{n_g^{eq}(\tau)} = \frac{n_g}{\frac{d_G}{\pi^2} T^3} = \frac{n_g}{\frac{d_G}{\pi^2} (e_g/3n_g)^3} = \lambda_0 \left( \frac{\tau_0}{\tau} \right)^{4-3\xi} \leq \lambda_0, \quad (50)$$

where  $\lambda_0 = \lambda(\tau_0)$ . The system will be continuously out of chemical equilibrium during the expansion, even if it is initially at local thermal equilibrium ( $\lambda_0 = 1$ ). The larger the viscosity, the smaller is the value of  $\xi$  and the faster is the decrease of the fugacity. Inclusion of production and annihilation processes such as the gluon bremsstrahlung and its back reaction ( $gg \leftrightarrow ggg$ ) makes chemical equilibration possible and thus, of course, Eq. (45) has to be modified! However, in this work we will use Eq.(45) without any modifications. The derivation of new and altered equations and their solutions will be given in a forthcoming publication [53].

One can solve Eqs. (46) and (47), if the initial values of  $n_g$ ,  $e_g$ ,  $\bar{\pi}_g$  and also the value of the shear viscosity  $\eta_g$  are given. On the other hand, to calculate  $\eta_g$  using Eq. (35) via Eq. (42) we need  $n_g$ ,  $e_g$ , and  $\bar{\pi}_g$ . It is obvious that an iterative algorithm has to be developed to calculate  $n_g$ ,  $e_g$ ,  $\bar{\pi}_g$  and  $\eta_g$  self-consistently. This algorithm is as follows:

1. We solve Eqs. (45)-(47) with a guessed value of  $\eta_g$ . The guessed value can be chosen arbitrarily because the final result does not depend on it.  $\eta_g/n_g$  is assumed to be a constant of time.
2. The obtained  $n_g(\tau)$ ,  $e_g(\tau)$  and  $\bar{\pi}_g(\tau)$  at a time  $\tau$  are used to calculate  $\eta_g(\tau)$  according to (35). We calculate first the moments  $P^{\mu\nu}$  using  $f(x, p)$  in Eq. (42) with given  $n_g(\tau)$ ,  $e_g(\tau)$  and  $\bar{\pi}_g(\tau)$ .
3. We turn back to step 1. The value of  $\eta_g(\tau)$  is used to solve Eqs. (46) and (47) again.

Iterations will continue, until the relative deviation of  $\eta_g$  from the previous one is sufficient small. The iterative procedure allows to calculate  $\bar{\pi}(\tau)$ ,  $e(\tau)$  and  $n(\tau)$  as well as  $\eta/s(\tau)$  in a consistent way for given interactions. We note that if  $\eta_g/n_g$  is strongly time dependent, further iterations will be required to account for this time dependence. A refined algorithm will be presented in [53].

To obtain  $\eta_g$ ,  $P^{\mu\nu}$  has to be first evaluated by (21) via (42).  $P^{\mu\nu}$  is a second moment of the collision term and thus is determined by gluon interactions considered. The compact forms of the collision terms can be found in [34]. In this article elastic ( $gg \rightarrow gg$ ) as well as bremsstrahlung ( $gg \leftrightarrow ggg$ ) processes inspired within perturbative QCD are responsible for the gluon dynamics. The differential cross section and the effective matrix element are taken as in Refs. [34, 39]:

$$\frac{d\sigma^{gg \rightarrow gg}}{dq_{\perp}^2} = \frac{9\pi\alpha_s^2}{(q_{\perp}^2 + m_D^2)^2}, \quad (51)$$

$$|\mathcal{M}_{gg \rightarrow ggg}|^2 = \frac{9g^4}{2} \frac{s^2}{(q_{\perp}^2 + m_D^2)^2} \frac{12g^2 \mathbf{q}_{\perp}^2}{\mathbf{k}_{\perp}^2 [(\mathbf{k}_{\perp} - \mathbf{q}_{\perp})^2 + m_D^2]} \Theta(k_{\perp} \Lambda_g - \cosh y) \quad (52)$$

where  $g^2 = 4\pi\alpha_s$ . The Debye screening mass

$$m_D^2 = d_G \pi \alpha_s \int dw N_c f(x, p) \quad (53)$$

with  $N_c = 3$  is applied to regularize infrared divergences. Although  $gg \leftrightarrow ggg$  processes are considered, they contribute only to the shear viscosity but not to chemical equilibration,

because as mentioned above, particle number conservation is assumed at present to derive Eq. (45)). Improvements will be done in a forthcoming publication [53].

## B. Results

Figure 1(a) shows  $\eta_g/s_g$  as a function of the expansion time for two values of the coupling constant  $\alpha_s = 0.05$  and  $0.3$ . The initial gluon system at  $\tau_0 = 0.4$  fm/c is assumed to be in thermal equilibrium with a temperature of  $T_0 = 500$  MeV. Each of the results indicated by the symbols in Fig. 1 is obtained by about 40 iterations with a guessed value of  $\eta_g(\text{guessed}) = 0.5 s_g^{eq}$ . From Fig. 1(a) we see that the ratio  $\eta_g/s_g$  is almost constant in time for  $\alpha_s = 0.3$ , whereas for  $\alpha_s = 0.05$ ,  $\eta_g/s_g$  increases moderately. The assumption underlying the iterative algorithm that  $\eta_g/n_g \approx 4\eta_g/s_g$  does not depend on time is justified accordingly. One finds that  $\eta_g/s_g \approx 0.18$  for a coupling of  $\alpha_s = 0.3$  and  $\eta_g/s_g \approx 3$  for  $\alpha_s = 0.05$ .

The results for the gluon fugacity (obtained from the solution of Eqs.(45)-(47)) depicted in Fig. 1(b) show a strong time dependence. The smaller the value of  $\alpha_s$ , i.e., the larger the  $\eta_g/s_g$ , the faster is the deviation from the chemical equilibrium. This quantitatively demonstrates the consideration from above [see Eqs. (50)].

When putting Eq. (42) into Eq. (21) one realizes that  $P^{\mu\nu} \sim \lambda^2 C_0 \bar{\pi} \sim \lambda \bar{\pi}$  in leading order of  $\bar{\pi}$ . Thus  $\eta_g$  does not depend on  $\lambda$ . Secondly, from Eq. (43) we obtain  $s_g/T^3 \sim \lambda(1 - \ln \lambda)$ . Thus,  $\eta_g/s_g \sim 1/\lambda(1 - \ln \lambda)$  and will increase slower than a logarithmical behavior when  $\lambda$  decreases: a stronger decrease of  $\lambda$  (comparing the result for  $\alpha_s = 0.05$  with that for  $\alpha_s = 0.3$  in the lower panel of Fig. 1) will lead to stronger increase of  $\eta_g/s_g$ , as seen in the numerical results shown in Fig. 1(a).

Figure 2(a) shows the deviation from kinetic equilibrium,  $\sigma_\phi$  from Eq. (44), as a function of time scaled with the initial time. For  $\alpha_s = 0.3$  the value of  $\sigma_\phi$  starts at zero (equilibrium), increases until  $3\tau_0$  and then relaxes to zero. The system first evolves out of equilibrium and then relaxes back to equilibrium. On the contrary,  $\sigma_\phi$  increases continuously when employing a much weaker (and unphysically low) coupling  $\alpha_s = 0.05$ . In this case the system is always out of equilibrium. To explain the different behaviors we define  $R_{OE}$  as the ratio of the mean transport free path,  $1/\sum R_{Grad}^{tr}$  defined by Eq. (40), to the Hubble-like expansion time scale  $\tau$ :

$$R_{OE} = \frac{\lambda^{tr}}{\tau} = \frac{1}{\tau \cdot \sum R_{Grad}^{tr}} \quad (54)$$

Our concept of  $R_{OE}$  is similar to that introduced in [37], where the authors demonstrate that the ratio of expansion time to the mean free path controls the deviation from equilibrium. For a fixed  $\eta_g/s_g$  the mean transport path  $\lambda^{tr} = 1/\sum R_{Grad}^{tr}$  changes with time. At full equilibrium  $\lambda^{tr} \sim 1/T \sim \tau^{1/3}$  and thus  $\lambda^{tr}/\tau \sim \tau^{-2/3}$ . If  $R_{OE}$  is larger than unity, the system starts to depart from equilibrium. If  $R_{OE}$  is smaller than unity, the system relaxes to equilibrium.  $R_{OE}(\tau)$  is shown in Fig. 2(b). With  $\alpha_s = 0.05$  the system evolves far away from equilibrium and the evolution is dominated by free streaming. The ratio  $R_{OE}$  is a measure of the ability of the system to relax to kinetic equilibrium. For  $\alpha_s = 0.05$  kinetic equilibration is not possible for the timescales shown. The regime for which the system can not come close to kinetic equilibrium is for the coupling  $\alpha_s = 0.1 - 0.2$  corresponding to a shear viscosity to entropy density ratio  $\eta/s = 0.8 - 0.4$ .

In addition,  $\sigma_\phi$  is larger than unity at  $\tau > 3\tau_0$  for  $\alpha_s = 0.05$ . The true entropy density  $s_g$  should be smaller than that estimated according to Eq. (43), because the expansion  $\ln(1 + \phi) \approx \phi$  is not valid any more for large  $\phi$ . The derivation of the shear viscosity in Eq. (35) becomes questionable as well, since the same expansion is used to obtain the entropy production (19).

Finally, in Figs. 3 and 4 we compare the results on  $\eta_g/s_g$  from the second-order (IS) kinetic theory with those presented in Ref. [12] using the Navier-Stokes approximation. The solid (dotted) curve in Fig. 3 depicts the contribution of  $gg \rightarrow gg$  ( $gg \leftrightarrow ggg$ ) to  $\eta_g/s_g$  obtained in [12]. The solid (dotted) curve with symbols depicts the results from the present calculations at  $\tau = 2\tau_0$ , at which the system is still near thermal equilibrium. We see that the results following from the second-order expansion are mostly larger than those based on the Navier-Stokes scheme, both for  $gg \rightarrow gg$  and for  $gg \leftrightarrow ggg$  processes. At (unphysical) small  $\alpha_s$  the difference between the results is given by a factor of 2 – 3. In particular, the difference between the second-order and the Navier-Stokes results for bremsstrahlung  $gg \leftrightarrow ggg$  is bigger than that for elastic  $gg \rightarrow gg$  process. At large  $\alpha_s$  the  $gg \leftrightarrow ggg$  processes play a dominant role (compared with  $gg \rightarrow gg$ ) in lowering  $\eta_g/s_g$ , whereas at small  $\alpha_s$  this dominance becomes weaker [11]. In Fig. 4 the results on  $\eta/s$  implementing both elastic and inelastic processes are shown for the physical region of  $\alpha_s$ . Here the difference between second-order and Navier-Stokes based calculations is approximately 50% ( $\alpha_s = 0.2$ )-20% ( $\alpha_s = 0.3$ )-0% ( $\alpha_s = 0.6$ ).

## V. CALCULATION OF SHEAR VISCOSITY IN A GLUON SYSTEM: TRANSPORT SIMULATIONS EMPLOYING BAMPS

In this section, we solve the Boltzmann equation for gluons using the parton cascade Boltzmann Approach of MultiParton Scatterings and repeat the task in the previous section to calculate the shear viscosity to entropy density ratio  $\eta_g/s_g$  in a Bjorken-type one-dimensional (0+1) expansion. We calculate  $\eta_g$  and  $s_g$  according to Eqs. (35) and (43) by extracting  $P^{\mu\nu}$ ,  $\bar{\pi}_g$ ,  $n_g$  and  $e_g$  from the transport simulations.

The partonic cascade BAMPS which was introduced in [34, 38] has been applied for a (0+1) dimensional expansion to study thermalization of a color glass condensate potentially produced in ultrarelativistic heavy ion collisions [39]. We take the same numerical setup for BAMPS as considered in [39]. The initial condition and interactions of gluons are the same as given in the previous section. In the parton cascade calculations, different from calculations using the viscous hydrodynamic equations (45)-(47), the inelastic  $gg \leftrightarrow ggg$  processes lead to a net particle production or absorption, i.e.,  $\partial_\mu N_g^\mu \neq 0$ , which drives the chemical equilibration.

We note that particle number changing processes are implemented in BAMPS, whereas the particle number was considered to be constant in previous section. Therefore we are not able to make a direct comparison between BAPMS results and those calculated by solving Israel-Stewart equations.

Figure 5 shows  $\eta_g/s_g$  extracted within the space time rapidity interval  $\eta_s \in [-0.1 : 0.1]$ , where  $\eta_s = \frac{1}{2} \ln[(t+z)/(t-z)]$ . When comparing these results with those shown in the upper panel of Fig. 1 we find that they are almost the same for  $\alpha_s = 0.3$ , whereas for  $\alpha_s = 0.05$  the increase of  $\eta_g/s_g$  is slightly weaker in BAMPS calculations than in viscous hydrodynamic ones. The reason for this difference is the different behavior of the gluon fugacity (remember that  $\eta_g/s_g \sim 1/\lambda(1 - \ln \lambda)$ ). The gluon fugacity extracted from BAMPS is shown in Fig. 6. Its value is larger than that shown in the lower panel of Fig. 1, because ongoing chemical equilibration is realized in the BAMPS calculations.

The kinetic equilibration is demonstrated in Fig. 7(a) via the variance  $\sigma_\phi$  and in Fig. 8 via the momentum isotropy  $Q(t) = \langle \frac{p_x^2}{E^2} \rangle$ . The results on  $\sigma_\phi$  are similar to those in Fig. 2 and can be well understood by the out-of-equilibrium ratio  $R_{OE}$  shown in Fig. 7(b). For  $\alpha_s = 0.3$  the transport mean free path is shorter than the expansion rate whereas for

$\alpha_s = 0.05$  the evolution is dominated by expansion. Momentum isotropization, shown in Fig. 8, is practically restored for  $\alpha_s = 0.3$  at later times, whereas for  $\alpha_s = 0.05$  this restoration is not possible. Here again the differences between transport and viscous hydrodynamic calculations stem from the different time evolution of the gluon fugacity. To make fair comparisons, modifications in the hydrodynamic equations will be done in the near future [53] to take into account the chemical equilibration.

As pointed out already in the previous section, the parameters for which the system cannot come close to kinetic equilibrium are the couplings of  $\alpha_s \approx 0.1 - 0.2$  corresponding to a ratio  $\eta/s \sim 0.8 - 0.4$ . For such parameters, the ratio  $\lambda^{tr}/\tau$  is of the order of 1 at late times and the system becomes highly diffusive and viscous.

Finally, in Fig. 9 we investigate deviations from equilibrium of the gluon distribution in BAMPS calculations at large momentum. Figure 9 shows the non-equilibrium part of the transverse spectrum (normalized to the equilibrium spectrum)  $\frac{dN/(p_T dp_T d\eta)}{dN_{eq}/(p_T dp_T d\eta)} - 1$  from BAMPS calculations and the quantity  $\langle \phi \rangle_{p_z}(\bar{\pi}, T, \lambda) = \int f_{eq} \phi(\bar{\pi}, T, \lambda) dp_z / \int f_{eq} dp_z$  [with  $\phi(x, p) = \frac{\pi^2}{8\lambda T^6} \bar{\pi}(p_z^2 - \frac{1}{2}p_T^2)$ ], which is the analytically calculated second-order contribution to the transverse spectrum, as a function of the transverse momentum  $p_T$  at  $\tau = 4\tau_0$ . The average  $\langle \phi \rangle_{p_z}$  is calculated using  $\bar{\pi}, T, \lambda$  extracted from the particular BAMPS calculations. The comparison of  $\frac{dN/(p_T dp_T d\eta)}{dN_{eq}/(p_T dp_T d\eta)} - 1$  and  $\langle \phi \rangle_{p_z}$  from Fig. 9 shows that for  $\alpha_s = 0.05$  the distribution function in BAMPS contains contributions higher order in  $p_T$  and  $\bar{\pi}$  and thus the second-order *ansatz* (17) is not sufficient to describe the evolution in BAMPS. In contrast, for  $\alpha_s = 0.3$  the distribution function is reasonably good approximated by second-order kinetic theory over the shown momentum range. Thus we argue that the dependence of  $\phi$  on  $\bar{\pi}/(\lambda T^4)$  is stronger than given by *ansatz* (17), since  $\bar{\pi}/(\lambda T^4) \sim \sigma_\phi$  quantifies the strength of dissipative effects, which are stronger at  $\alpha_s = 0.05$ . Inclusion of additional terms in Eq. (17) would lead to a modification of the evolution equation for  $\bar{\pi}$ , which follows from the conservation law for the energy momentum tensor:  $0 = \partial_\mu T^{\mu\nu} \sim \partial_\mu \int p^\mu p^\nu f_{eq}(1 + \phi)$ . If employing  $\alpha_s = 0.05(\eta/s \approx 3)$  for large  $p_T > 2.3$  GeV the variance  $\langle \phi \rangle_{p_z}$  becomes larger than 1. For  $\alpha_s = 0.3$  this happens at  $p_T > 2.75$  GeV. For transverse momenta larger than these critical values the expansion  $\ln(1 + \phi) \approx \phi$  done to obtain Eq.(19) is invalidated. Thus in the calculation of the entropy density (and entropy production) the  $\ln(1 + \phi)$  term should be approximated by  $\ln(1 + \phi) \approx \phi - \frac{\phi^2}{2} \Theta(p_T - p_{Tcrit})$ , i.e. higher order terms should be taken into account in the integration over the momentum for  $p_T > p_{Tcrit}$ .



However, with  $\eta/s = 0.18$  this correction is less than 0.5%, which is due to the smallness of  $\sigma_\phi$ . With  $\eta/s = 3$  the correction is  $\sim 6\%$ . Thus for physical values of  $\eta/s \sim 0.2$  second-order hydrodynamics is valid, even though *formally* breaking down at large  $p_T$ . In the unphysical regime  $\eta/s \sim 3$  higher order corrections are not negligible. This deserves future investigation [53].

## VI. CONCLUSIONS

We have derived the shear viscosity coefficient  $\eta$  from kinetic theory for massless particle system undergoing a one-dimensional expansion with Bjorken boost-invariance. The derivation makes use of Grad's moment method [45, 47] and is based on an expansion of the distribution function up to second order in momentum. The final expression obtained in the present work is similar to the one based on the Navier-Stokes theory [12], but the transport rate has to be calculated in a different way. How close the result obtained using Grad's method approximates the true value determined using the Kubo-Green formula [54] will be studied and reported in a forthcoming publication. The values needed to calculate the shear viscosity [Eq. (35)] are shear tensor  $\pi_{\mu\nu}$ , the particle and energy densities  $e$  and  $n$ , the fugacity  $\lambda$  and finally the second moments  $P_{\mu\nu}$  of the collision term from the underlying kinetic process. They can be calculated either using transport setup solving the kinetic theory or from dissipative hydrodynamic (Israel-Stewart) equations (45)-(47). However, the IS equations themselves need the value of shear viscosity as a parameter. Thus we introduce a new iterative method that allows us to solve Israel-Stewart equations and calculate  $\eta/s$  as a function of time and coupling constant  $\alpha_s$ . The results on  $\eta/s$  calculated in the partonic cascade BAMPS and from IS theory are in a good agreement for physical coupling  $\alpha_s = 0.3$ . In this regime we obtain  $\eta/s = 0.18$ . As a further demonstration even for unphysical small coupling  $\alpha_s = 0.05$  the difference between BAMPS and second-order hydrodynamic calculations of  $\eta/s$  is small. We obtain  $\eta/s \approx 3$  in this regime. At such small coupling  $\eta/s$  increases slightly in BAMPS and somewhat stronger in hydrodynamic calculations. This increase is due to the intrinsic fugacity, which evolves differently in both calculations.

Using IS theory, we calculate  $\eta/s$  ratio for a system close to equilibrium as a function of  $\alpha_s$ . For physical coupling  $\alpha_s \approx 0.3$  the second-order result is approximately 20% higher than in calculations based on first order Navier-Stokes theory [12]. For  $\alpha_s = 0.6$   $\eta/s = 0.08$

within the Israel-Stewart and Navier-Stokes prescription.

Deviations of hydrodynamic evolution from equilibrium are quantified in the present work introducing the variance  $\sigma_\phi$  of the nonequilibrium part of the distribution function. We demonstrate that its value is smaller than unity and later decreases with time at a physical coupling  $\alpha_s = 0.3$  and thus our expression of  $\eta$  is valid in this case. Here again hydrodynamic and BAMPS results are in good agreement. For small coupling  $\alpha_s = 0.05$  hydrodynamics does not relax back to equilibrium and Grad's method becomes invalid. In BAMPS in this regime the deviation of  $\sigma_\phi$  from equilibrium is smaller, which is an effect of the ongoing chemical equilibration. The ability of the system to restore kinetic equilibrium is quantified by the ratio of the mean transport free path to the expansion time. We conclude that the second-order dissipative hydrodynamics is applicable in the regime  $\eta/s \lesssim 0.2$  which corresponds to values of  $\alpha_s \gtrsim 0.3$ . At high momenta  $p_T > 3$  GeV it formally breaks down, however for  $\eta/s \sim 0.2 - 0.4$  it is applicable even for differential observables. For really high  $\eta/s \sim 3$  the applicability of hydrodynamics certainly breaks down. For the intermediate regime  $0.3 < \eta/s < 0.8$  a more detailed analysis in the comparison of microscopic transport description to dissipative second- (or even higher) order hydrodynamics is required.

To make consistent comparisons between the kinetic transport model BAMPS and IS solutions we have to modify the hydrodynamic equation to take into account particle production and absorption. These calculations will be reported in a forthcoming publication.

## Acknowledgments

The authors thank D. H. Rischke and B. Betz for helpful discussions.

A. E. gratefully acknowledges a fellowship by the Helmholtz foundation. This work is supported by BMBF and by the Helmholtz International Center for FAIR within the framework of the LOEWE program (LandesOffensive zur Entwicklung Wissenschaftlich-ökonomischer Exzellenz) launched by the State of Hesse. A. M. acknowledges the support by the National Research Foundation under Grant No. (NRF GUN 61698).

The BAMPS simulations were performed at the Center for Scientific Computing of Goethe

University.

---

- [1] K. H. Ackermann et al. [STAR Collaboration], Phys. Rev. Lett. **86** (2001) 402; C. Adler et al. [STAR Collaboration], ibid. **87** (2001) 182301; **89** (2002) 132301; Phys. Rev. C **66** (2002) 034904; J. Adams et al. [STAR Collaboration], nucl-ex/0409033; J. Adams et al. [STAR Collaboration], Phys. Rev. Lett. **92** (2004) 052302.
- [2] K. Adcox et al. [PHENIX Collaboration], Phys. Rev. Lett. **89** (2002) 212301; S. S. Adler et al. [PHENIX Collaboration], ibid. **91** (2003) 182301;
- [3] B. B. Back et al. [PHOBOS Collaboration], Phys. Rev. Lett. **89** (2002) 222301; nucl-ex/0406021; nucl-ex/0407012.
- [4] T. D. Lee, Nucl. Phys. A **750** (2005) 1.
- [5] M. Gyulassy, L. McLerran, Nucl. Phys. A **750** (2005) 30.
- [6] E. V. Shuryak, Nucl. Phys. A **750** (2005) 64.
- [7] P. Huovinen, P.F. Kolb, U. W. Heinz, H. Heiselberg, Phys. Lett. B **500** (2001) 232.
- [8] G. Baym, H. Monien, C. J. Pethick and D. G. Ravenhall, Phys. Rev. Lett. **64** (1990) 1867.
- [9] A. Hosoya, K. Kajantie, Nucl. Phys. B **250** (1985) 666.
- [10] H. Heiselberg, Phys. Rev. D **49** (1994) 4739.
- [11] P. Arnold, G. D. Moore, L. G. Yaffe, J. High Energy Phys. **11** (2000) 001; J. High Energy Phys. **0305** (2003) 051.
- [12] Z. Xu, C. Greiner, Phys. Rev. Lett. **100** (2008) 172301.
- [13] T. Hirano, M. Gyulassy, Nucl. Phys. A **769** (2006) 71.
- [14] H. B. Meyer, Phys. Rev. D **76** (2007) 101701(R).
- [15] P. K. Kovtun, D. T. Son, A. O. Starinets, Phys. Rev. Lett. **94** (2005) 111601.
- [16] T. Koide, E. Nakano, T. Kodama, arXiv:0901.3707
- [17] R. Baier, P. Romatschke, Eur. Phys. J. C **51** (2007) 677.
- [18] D. Teaney, Phys. Rev. C **68** (2003) 034913.
- [19] U. W. Heinz, H. Song, A. K. Chaudhuri, Phys. Rev. C **73** (2006) 034904.
- [20] H. Song, U.W. Heinz, Phys. Rev. C **77** (2008) 064901.
- [21] C. E. Aguiar, T. Kodama, T. Osada, Y. Hama, J. Phys. G **27** (2001) 75.
- [22] A. Muronga, Phys. Rev. C **76** (2007) 014909.

- [23] J. Brachmann, A. Dumitru, J. A. Maruhn, H. Stöcker, W. Greiner, D. H. Rischke, Nucl. Phys. A **619** (1997) 391.
- [24] K. Dusling, D. Teaney, Phys. Rev. C **77** (2008) 034905
- [25] W. Israel, Ann. Phys. (N.Y.) **100** (1976) 310;  
J.M. Stewart, Proc. R. Soc. London , Ser. A **357** (1977) 59;  
W. Israel, M. Stewart, Ann. Phys. (N.Y.) **118** (1979) 341
- [26] M. Luzum, P. Romatschke, Phys. Rev. C **78** (2008) 034915.
- [27] P. Romatschke, U. Romatschke, Phys. Rev. Lett. **99** (2007) 172301.
- [28] T. Hirano, U. W. Heinz, D. Kharzeev, R. Lacey, Y. Nara, Phys. Lett. B **636** (2006) 299.
- [29] K. Geiger, B. Müller, Nucl. Phys. B **369** (1992) 600.
- [30] B. Zhang, Comput. Phys. Commun. **109** (1998) 193; **111** (1998) 276(E).
- [31] D. Molnar, M. Gyulassy, Phys. Rev. C **62** (2000) 054907.
- [32] V. Borchers, J. Meyer, S. Gieseke, G. Martens, C. C. Noack, Phys. Rev. C **62** (2000) 064903.
- [33] S. A. Bass, B. Müller, D. K. Srivastava, Phys. Lett. B **551** (2003) 277.
- [34] Z. Xu, C. Greiner, Phys. Rev. C **71** (2005) 064901.
- [35] L. W. Chen, V. Greco, C. M. Ko, and P. F. Kolb, Phys. Lett. B **605** (2005) 95.
- [36] M. Bleicher et al., J. Phys. G **25** (1999) 1859.
- [37] P. Huovinen, D. Molnar , arXiv:0808.0953
- [38] Z. Xu, C. Greiner, Phys. Rev. C. **76** (2007) 024911.
- [39] A. El, Z. Xu, C. Greiner, Nucl. Phys. A **806** (2008) 287.
- [40] Z. Xu, C. Greiner, H. Stocker, Phys. Rev. Lett. **101** (2008) 082302.
- [41] Z. Xu, C. Greiner, arXiv:0811.2940v1 .
- [42] Z. Xu, C. Greiner, H. Stocker, arXiv:0807.2986v1.
- [43] O. Fochler, A. El, Z. Xu, C. Greiner, arXiv:0810.5667v1 .
- [44] I. Bouras, 'Stosswellenphänomene in einer partonischen Kaskade', master thesis, Frankfurt am Main (2008);  
I. Bouras et al., arXiv:0811.4133v1 .
- [45] A. Muronga, Phys. Rev. C **76** (2007) 014910.
- [46] J. D. Bjorken, Phys. Rev. D **27** (1983) 140 .
- [47] H. Grad, Commun. Pure Appl. Math. **2** (1949) 331 .
- [48] D. H. Rischke, PhD thesis, Frankfurt, (1993) (unpublished)

- [49] S. R. de Groot, W. A. van Leeuwen, Ch. G. van Weert,  
Relativistic Kinetic Theory: Principles and Applications  
(North Holland, Amsterdam, 1980).
- [50] H.-Th. Elze, J. Rafelski, L. Turko, Phys. Lett. B **506** (2001) 123.
- [51] A. Muronga, Phys. Rev. C **69** (2004) 034903.
- [52] R. Baier, P. Romatschke, U. A. Wiedemann, Phys. Rev. C **73** (2006) 064903.
- [53] A. El, Z. Xu, C. Greiner, in preparation.
- [54] N. Demir, S. A. Bass, arXiv:0812.2422

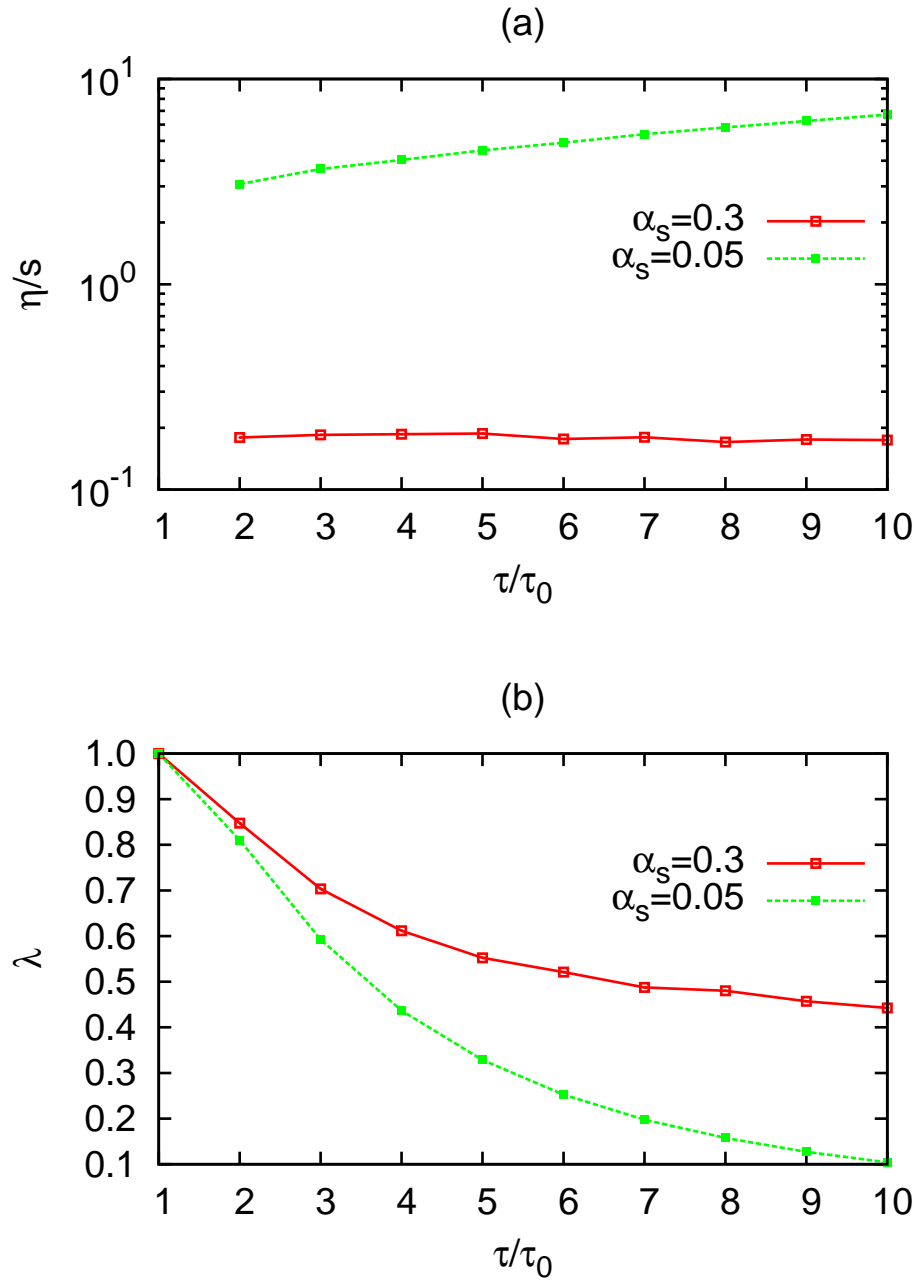


FIG. 1: (Color online) (a)  $\eta/s$  ratio and (b) fugacity  $\lambda$  calculated by the iterative procedure described in the text for  $\alpha_s = 0.05$  and  $\alpha_s = 0.3$  at ten different time points, with initial time  $\tau_0 = 0.4$  fm/c,  $T(\tau_0) = 500$  MeV. The initial input value of  $\eta/s$  is 0.5.

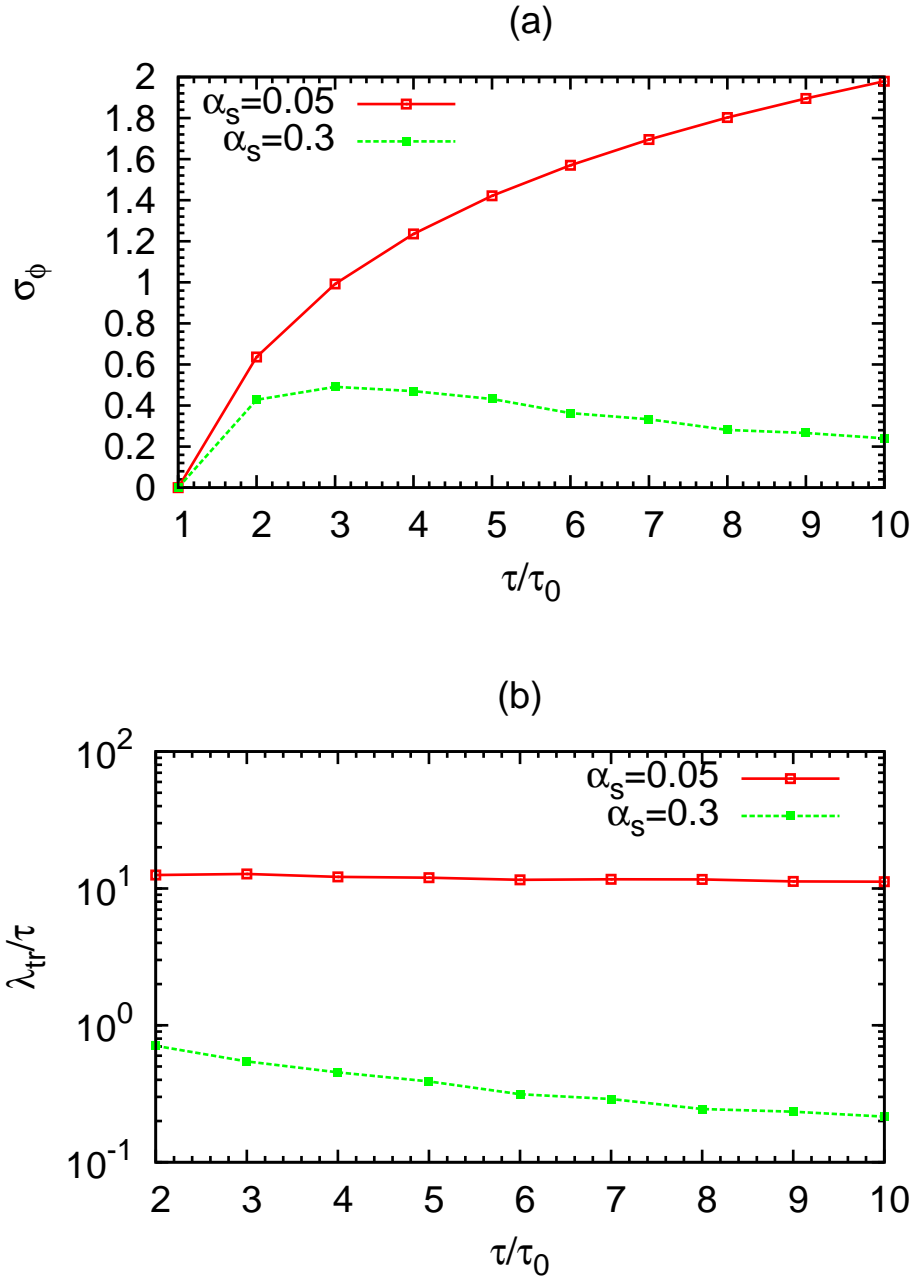


FIG. 2: (Color online) (a) Variance  $\sigma_\phi$  and (b) ratio  $R_{OE}$  calculated by the iterative procedure.  $\tau_0 = 0.4 \text{ fm}/c$ .

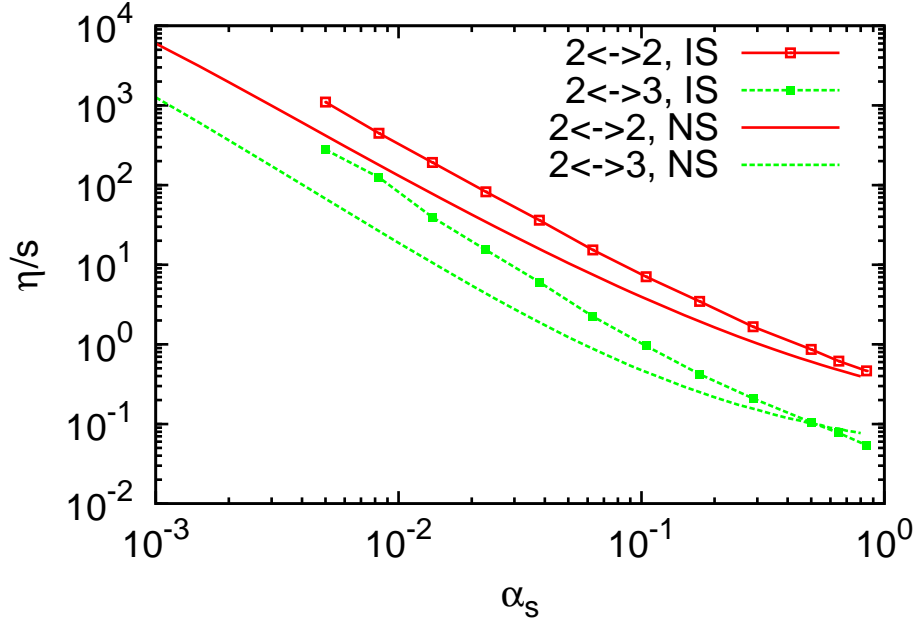


FIG. 3: (Color online) Ratio  $\eta/s$  (contributions due to elastic and inelastic processes) as function of the coupling constant  $\alpha_s$ . The result (solid line) is compared with results of Ref. [12] (dotted line)

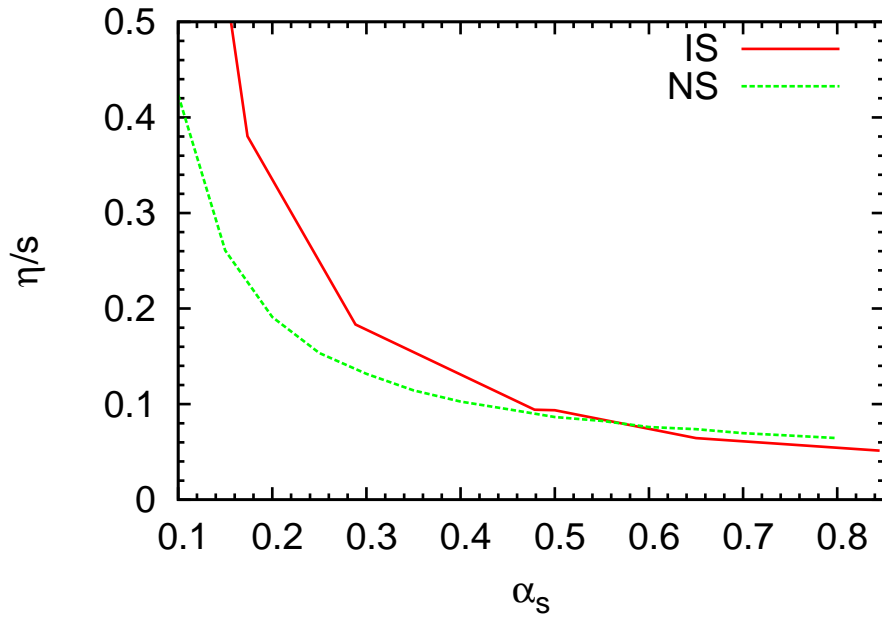


FIG. 4: (Color online) Ratio  $\eta/s$  (all processes) as function of the coupling constant  $\alpha_s$ . The result is compared with result of Ref. [12]



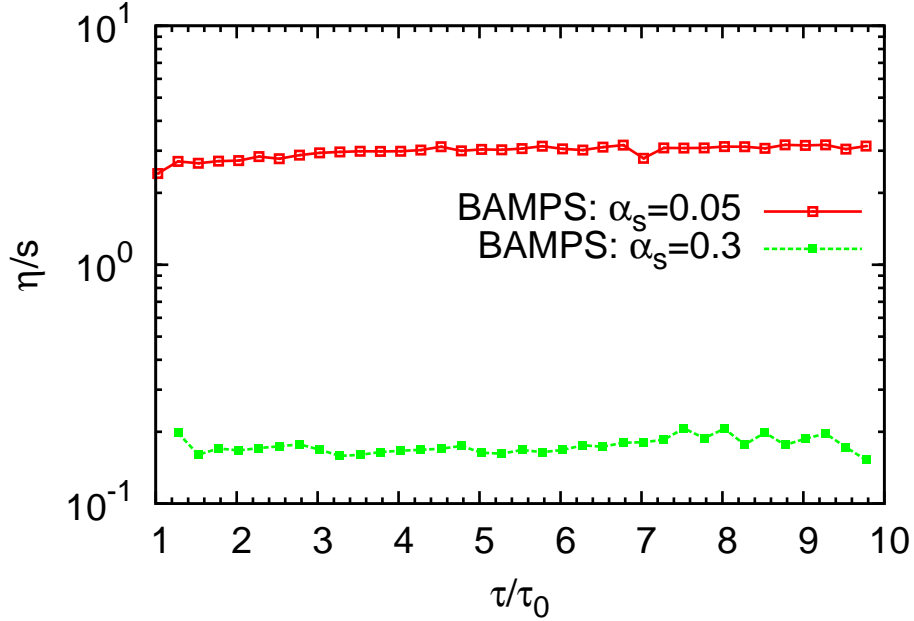


FIG. 5: (Color online) Ratio  $\eta/s$  from the microscopic BAMPS simulation. Results are calculated using Eq. (35) for simulations with two different values for  $\alpha_s$ .  $\tau_0 = 0.4 \text{ fm}/c$

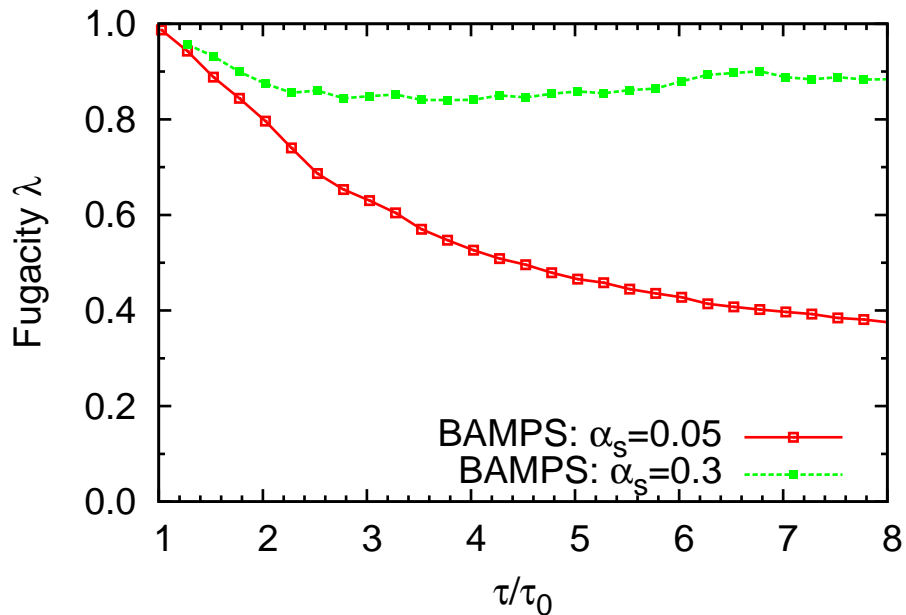


FIG. 6: (Color online) Fugacity  $\lambda = n/n_{eq}$  from BAMPS calculation. Results are shown for simulations with different (constant) values of  $\alpha_s$ .  $\tau_0 = 0.4 \text{ fm}/c$ .

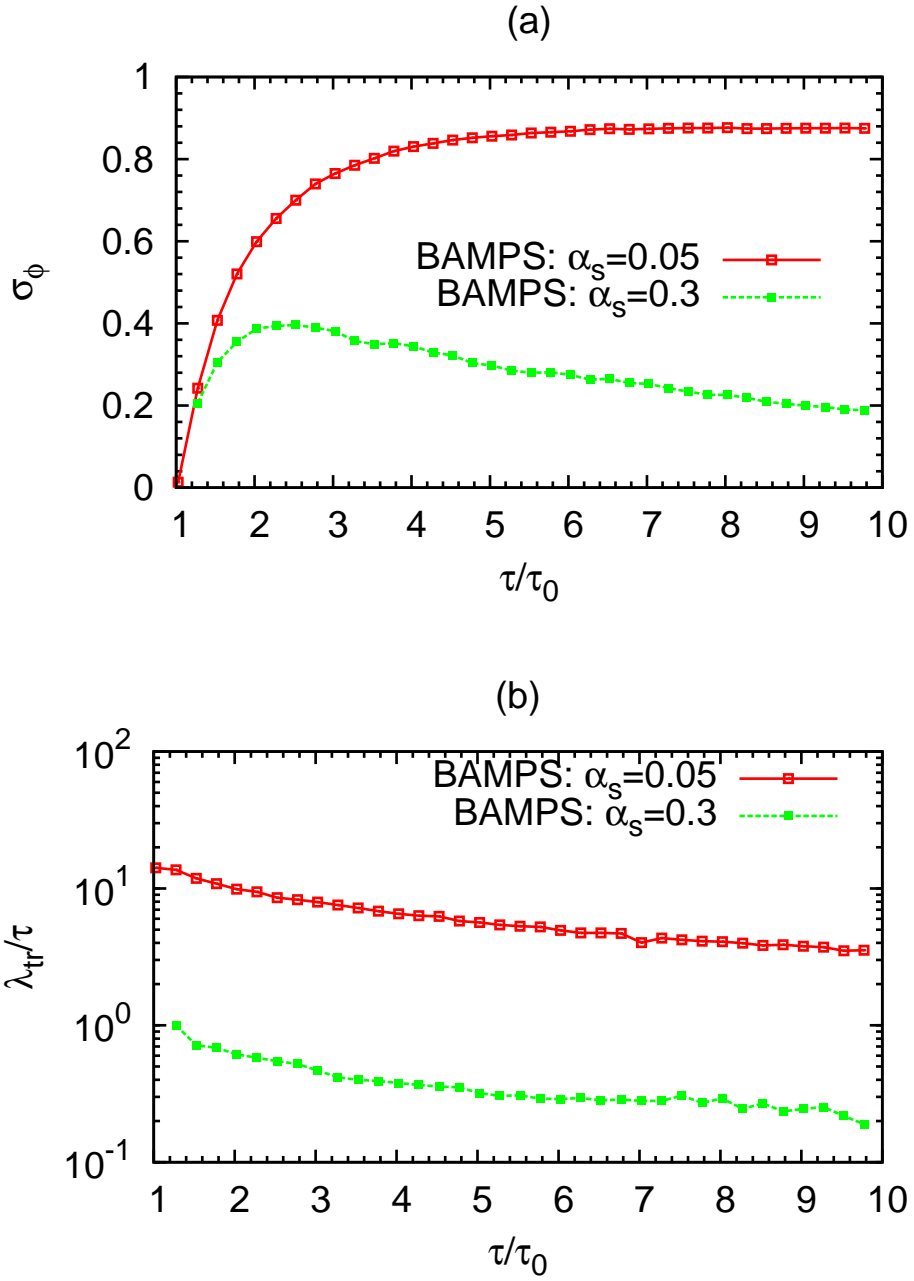


FIG. 7: (Color online) (a) Variance  $\sigma_\phi$  and (b) ratio  $R_{OE}$  calculated by BAMPS.  $\tau_0 = 0.4$  fm/c.

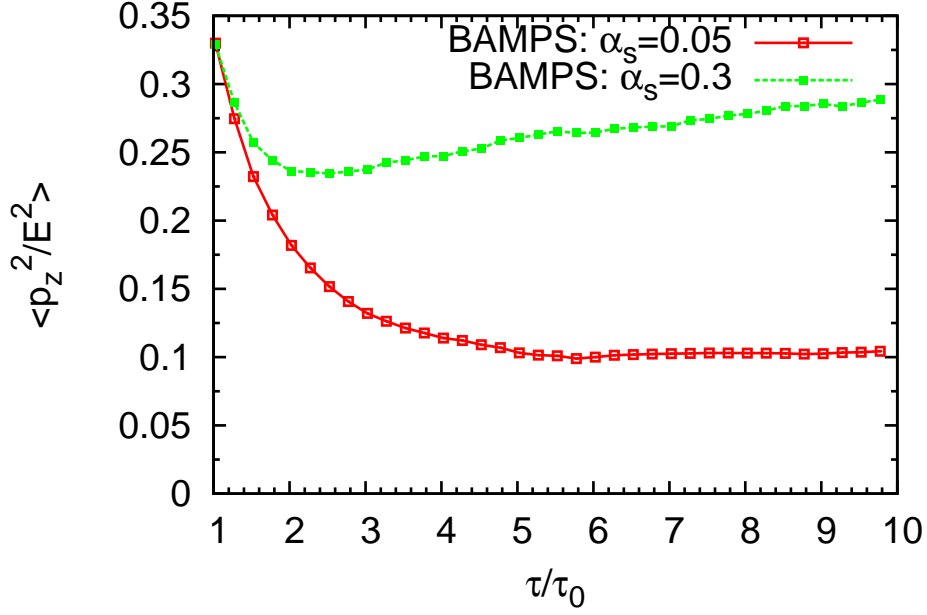


FIG. 8: (Color online) Momentum isotropy  $\langle p_z^2/E^2 \rangle$  calculated by BAMPS.  $\tau_0 = 0.4$  fm/c.

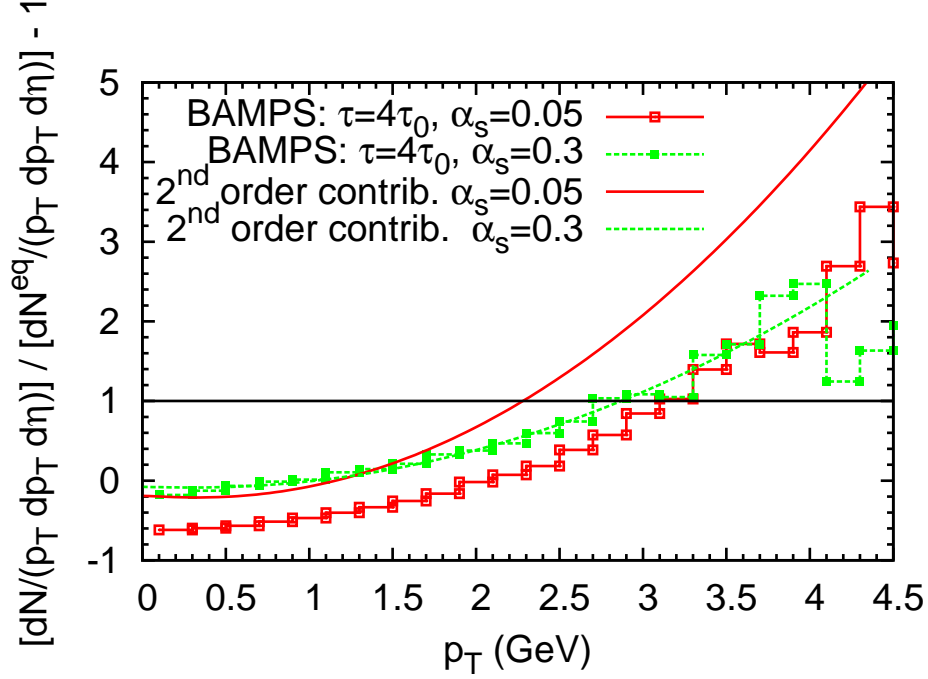


FIG. 9: (Color online) Nonequilibrium part of the transverse spectrum (normalized to the equilibrium spectrum)  $\frac{dN/(p_T dp_T d\eta)}{dN_{eq}/(p_T dp_T d\eta)} - 1$  from BAMPS calculations (lines with points) and the second-order contribution to the transverse spectrum  $\frac{\int f_{eq} \phi(\pi, T, \lambda) dp_z}{\int f_{eq} dp_z}$  (lines) as function of  $p_T$  at  $\tau = 4\tau_0$  with  $\bar{\pi}, T, \lambda$  extracted from BAMPS.